Rotational excitation of ortho-H2O by para-H2 (j2 = 0, 2, 4, 6, 8) at high temperature

Marie-Lise Dubernet-Tuckey, Fabien Daniel, A. Grosjean, C. Y. Lin

A&A 497, 911–925 (2009)
DOI: 10.1051/0004-6361/200810680

Astronomy & Astrophysics

Rotational excitation of ortho-H_2O by para-H_2 ($j_2 = 0, 2, 4, 6, 8$) at high temperature

M.-L. Dubernet[1,2], F. Daniel[2,3], A. Grosjean[4], and C. Y. Lin[2]

[1] Université Pierre et Marie Curie, LPMAA UMR CNRS 7092, Case 76, 4 place Jussieu, 75252 Paris Cedex 05, France
e-mail: marie-lise.dubernet@obspm.fr
[2] Observatoire de Paris-Meudon, LERMA UMR CNRS 8112, 5 place Jules Janssen, 92195 Meudon Cedex, France
[3] Departamento Molecular and Infrared Astrophysics, Consejo Superior de Investigaciones Cientificas, C/ Serrano 121, 28006 Madrid, Spain
[4] Institut UTINAM, UMR CNRS 6213, 41bis avenue de l'Observatoire, BP 1615, 25010 Besançon Cedex, France

Received 25 July 2008 / Accepted 17 December 2008

ABSTRACT

Aims. Our objective is to obtain the best possible set of rotational (de)-excitation state-to-state and effective rate coefficients for temperatures up to 1500 K. We present state-to-state rate coefficients among the 45 lowest levels of o-H_2O with $H_2(j_2 = 0)$ and $\Delta j_2 = 0, +2$, as well as with $H_2(j_2 = 2)$ and $\Delta j_2 = 0, -2$. In addition and only for the 10 lowest energy levels of o-H_2O, we provide state-to-state rate coefficients involving $j_2 = 4$ with $\Delta j_2 = 0, -2$ and $j_2 = 2$ with $\Delta j_2 = +2$. We give estimates of effective rate coefficients for $j_2 = 6, 8$.
Methods. Calculations are performed with the close coupling (CC) method over the whole energy range, using the same 5D potential energy surface (PES) as the one employed in our latest publication on water. We perform comparisons with coupled states (CS) calculations, with thermalized quasi-classical trajectory (QCT) calculations using the same PES and with previous quantum calculations obtained between $T = 20$ K and $T = 140$ K with a different PES.
Results. We find that the CS approximation fares extremely badly even at high energy for j_2 different from zero. Comparisons with thermalized QCT calculations show large factors at intermediate temperatures and factors from 1 to 3 at high temperature for the strongest rate coefficients. Finally we stress that scaled collisional rate coefficients obtained with He cannot be used in place of collisional rate coefficients with H_2.

Key words. molecular data – molecular processes – ISM : molecules

1. Introduction

This is the first effort on such a large scale to obtain the highest possible accuracy for collisional excitation rate coefficients of an asymmetric molecule with a rotationally excited diatomic molecule. This effort is justified by the importance of water in various astrophysical media. Water is a key molecule for the chemistry and the energy balance of the gas in cold clouds and star forming regions, thanks to its relatively large abundance and large dipole moment. A wealth of observational data has been obtained by the Infrared Space Observatory (see for example: Cernicharo & Crovisier 2005; Spinoglio et al. 2001; Tsuji 2001; Wright et al. 2000), the Submillimeter Wave Astronomy Satellite (Melnick et al. 2000) and the ODIN satellite (Sandqvist et al. 2003; Wilson et al. 2003). In the near future the Heterodyne Instrument for the Far-Infrared (HIFI) will be launched on board the Herschel Space Observatory. It will observe with unprecedented sensitivity spectra of many molecules with an emphasis on water lines in regions such as low or high mass star forming regions, proto-planetary disks and AGB stars. The interpretation of these spectra will rely upon the accuracy of the available collisional excitation rate coefficients that enter into the population balance of the emitting levels of the molecules. In the temperature range from 5 K to 1500 K, the most abundant collider likely to excite molecules in media with weak UV radiation fields is the hydrogen molecule, followed by the helium atom.

A pioneering rigid-body 5D PES was obtained by Phillips et al. (1994) for the excitation of the rotational levels of H_2O by H_2. Using this PES, Phillips et al. (1996) computed rate coefficients for rotational de-excitation among the first 5 ortho and para levels of water with H_2 ($j = 0, 1$) for temperatures ranging from 20 K to 140 K. Dubernet & Grosjean (2002) and Grosjean et al. (2003) extended this work down to 5 K and pointed out that such low temperature rates are highly sensitive to a proper description of resonances.

Recently an accurate 9D PES for the deformable $H_2 - H_2O$ system was calculated by Faure et al. (2005a). This PES combined conventional 5D and 9D CCSD(T) calculations (coupled cluster with perturbative triples) and accurate calibration data using the explicitely correlated CCSD(T)-R12 approach (Noga & Kutzelnigg 1994).

As a first application of the 9D PES, high temperature ($1500 \text{ K} < T < 4000$ K) rate coefficients for the relaxation of the ν_2 bending mode of H_2O were estimated from quasiclassical trajectory calculations (Faure et al. 2005a) and the role of rotation in the vibrational relaxation of water was emphasized (Faure et al. 2005b).

Another application of this 9D PES was to construct an accurate 5D PES suitable for inelastic rotational calculations by averaging over H_2 and H_2O ground vibrational states. As was pointed out in Faure et al. (2005a), this state-averaged PES is actually very close to a rigid-body PES using state-averaged geometries for H_2O and H_2.

Using this newly determined 5D PES for H_2–H_2O, Dubernet et al. (2006b) provided an extended and revised set of rate coefficients for de-excitation of the lowest 10 rotational levels of o/p-H_2O by collisions with p-H_2 ($j_2 = 0$) and o-H_2($j_2 = 1$), for kinetic temperatures from 5 K to 20 K.

The new PES of Faure et al. (2005a) leads to a significant re-evaluation of the rate coefficients for the excitation of H_2O by para-H_2 ($j = 0$). Indeed for the 1_{10} to 1_{01} transition observed by the SWAS satellite, the new PES increases the de-excitation rate coefficient by a factor of 4 at 5 K and by 75% at 20 K compared to the previous results of Dubernet et al. (Dubernet & Grosjean 2002; Grosjean et al. 2003), leading to a total increase at 20 K of 185% with respect to the Phillips et al. (1996) results. The de-excitation rate coefficients of other transitions induced by para-H_2 can increase by as much as 100% or decrease by 30%. For collisions with ortho-H_2($j = 1$) the new PES has a smaller effect on the de-excitation rate coefficients with a maximum change of 40%. The influence of the new PES on collisions with both p-H_2 ($j_2 = 0$) and o-H_2 ($j_2 = 1$) is expected to become less pronounced at higher temperatures.

Faure et al. (2007) provided rate coefficients for rotational de-excitation among the lowest 45 rotational levels of o/p-H_2O colliding with o/p-H_2 in the temperature range 20–2000 K. This set is a combination of various data: 1) data obtained with quasi classical trajectory (QCT) calculations with the H_2 molecule assumed to be rotationally thermalized at kinetic temperature and calculated between 100 K and 2000 K; 2) the values at 20 K are CC calculations from Dubernet et al. (2006b) for the first 5 levels and are equal to values at 100 K for all other levels; 3) scaled H_2O-He results from Green et al. (1993) for the weakest rate coefficients. A preliminary comparison (Faure et al. 2007) with current CC calculations concerning low lying levels of water at high temperature showed that QCT thermalized rate coefficients were accurate to within a factor of 1–3 for the dominant transitions, i.e. for those with rates larger than a few 10^{-12} cm^3 s^{-1}.

Our current objective is to obtain the best possible set of rotational (de)-excitation state-to-state and effective rate coefficients for temperatures up to 1500 K. We provide state-to-state rate coefficients among the 45 lowest levels of o-H_2O with $H_2(j_2 = 0)$ and $\Delta j_2 = 0, +2$, as well as with $H_2(j_2 = 2)$ and $\Delta j_2 = 0, -2$. In addition and only for the 10 lowest energy levels of o-H_2O, we provide state-to-state rate coefficients involving $j_2 = 4$ with $\Delta j_2 = 0, -2$ and $j_2 = 2$ with $\Delta j_2 = +2$. We give estimates of effective rate coefficients for $j_2 = 6, 8$.

2. Methodology

2.1. Collisions with H_2

Our calculations provide state-to-state collisional rate coefficients involving changes in both the target and the perturber rotational levels, i.e. $R(j_1\tau_1 j_2 \rightarrow j'_1\tau'_1 j'_2)(T)$ where $j_1\tau_1$, $j'_1\tau'_1$ represent the initial and final rotational levels of water, j_2, j'_2 the initial and final rotational levels of H_2, and T is the kinetic temperature.

The state-to-state collisional rate coefficients are the Boltzmann thermal averages of the state-to-state inelastic cross sections:

$$R(j_1\tau_1 j_2 \rightarrow j'_1\tau'_1 j'_2)(T) = \left(\frac{8}{\pi\mu}\right)^{1/2} \frac{1}{(k_B T)^{3/2}} \int_0^\infty \sigma_{j_1\tau_1 j_2 \rightarrow j'_1\tau'_1 j'_2}(E)\, E\, e^{-E/k_B T} dE, \quad (1)$$

where E is the kinetic energy, k_B is the Boltzmann constant and μ is the reduced mass of the colliding system.

These state-to-state collisional rate coefficients follow the detailed balance principle and reverse rate coefficients $R(j'_1\tau'_1 j'_2 \rightarrow j_1\tau_1 j_2)(T)$ can be obtained from forward rate coefficients by the usual formula:

$$g_{j'_1} g_{j'_2} e^{-\frac{E'_{int}(H_2O)}{k_B T}} e^{-\frac{E'_{int}(H_2)}{k_B T}} R(j'_1\tau'_1 j'_2 \rightarrow j_1\tau_1 j_2) = g_{j_1} g_{j_2} e^{-\frac{E_{int}(H_2O)}{k_B T}} e^{-\frac{E_{int}(H_2)}{k_B T}} R(j_1\tau_1 j_2 \rightarrow j'_1\tau'_1 j'_2), \quad (2)$$

where g_{j_1}, g_{j_2} are the statistical weights related to rotational levels of H_2O and H_2 respectively, and the different E_{int} are the rotational energies of the species.

Some astrophysical applications might rather use the so-called effective rate coefficients $\hat{R}_{j_2}(j_1\tau_1 \rightarrow j'_1\tau'_1)$ which are given by the sum of the state-to-state rate coefficients (Eq. (1)) over the final j'_2 states of H_2 for a given initial j_2:

$$\hat{R}_{j_2}(j_1\tau_1 \rightarrow j'_1\tau'_1)(T) = \sum_{j'_2} R(j_1\tau_1 j_2 \rightarrow j'_1\tau'_1 j'_2)(T). \quad (3)$$

These effective rate coefficients do not follow the detailed balance principle and both excitation and de-excitation should be explicitly calculated. It should be recalled that in the temperature range between 5 K and 20 K (Dubernet & Grosjean 2002; Grosjean et al. 2003), the effective rate coefficients follow the principle of detailed balance within the calculation error, because there are no transitions to the $j_2 = 3$ rotational level of o-H_2, and transitions to the $j_2 = 2$ rotational level of p-H_2 are negligeable.

Finally, averaged de-excitation rate coefficients for o/p-H_2O by rotationally thermalized o/p-H_2 can be obtained by averaging over the initial rotational levels of o/p-H_2:

$$\overline{R}(j_1\tau_1 \rightarrow j'_1\tau'_1) = \sum_{j_2} \rho(j_2) \hat{R}_{j_2}(j_1\tau_1 \rightarrow j'_1\tau'_1)(T) = \sum_{j_2} \rho(j_2) \sum_{j'_2} R(j_1\tau_1 j_2 \rightarrow j'_1\tau'_1 j'_2)(T) \quad (4)$$

with $\rho(j_2) = g_{j_2} e^{-\frac{E_{int}(H_2)}{k_B T}}/Z$, where Z is the partition function over either ortho or para-H_2 states. These averaged de-excitation rate coefficients are those directly calculated by Faure et al. (2007) with a QCT method.

2.2. Description of the calculations

In the current calculations we use the same expansion of the Faure et al. (2005a) 5D PES as in Dubernet et al. (2006b), where details can be found. For this PES, inaccuracies in inelastic cross sections might come from different sources: propagation parameters, description of the rotational Hamiltonians of the 2 molecules, sizes of H_2O and H_2 rotational basis sets,

Table 1. Energy levels of o-water obtained with the Kyrö (1981) Hamiltonian.

Level	Energy (cm^{-1})	j	τ	k_a	k_c	Level	Energy (cm^{-1})	j	τ	k_a	k_c
1	23.7943	1	–1	0	1	24	744.1639	8	–7	1	8
2	42.3717	1	1	1	0	25	756.7256	6	1	4	3
3	79.4963	2	–1	1	2	26	782.4112	7	–3	2	5
4	134.9018	2	1	2	1	27	842.3574	7	–1	3	4
5	136.7617	3	–3	0	3	28	885.6018	8	-5	2	7
6	173.3656	3	–1	1	2	29	888.5995	6	3	5	2
7	212.1561	3	1	2	1	30	920.1698	9	–9	0	9
8	224.8383	4	–3	1	4	31	931.2383	7	1	4	3
9	285.4192	3	3	3	0	32	1006.1173	8	–3	3	6
10	300.3621	4	–1	2	3	33	1045.0572	6	5	6	1
11	325.3483	5	–5	0	5	34	1059.8371	7	3	5	2
12	382.5171	4	1	3	2	35	1079.0815	9	–7	1	8
13	399.4581	5	–3	1	4	36	1114.5515	10	–9	1	10
14	446.5107	5	–1	2	3	37	1122.7100	8	–1	4	5
15	447.2528	6	–5	1	6	38	1201.9234	9	–5	2	7
16	488.1084	4	3	4	1	39	1216.1956	7	5	6	1
17	508.8121	5	1	3	2	40	1255.1688	8	1	5	4
18	552.9119	6	–3	2	5	41	1282.9207	9	–3	3	6
19	586.2445	7	–7	0	7	42	1293.6356	10	–7	2	9
20	610.3418	5	3	4	1	43	1327.1114	11	–11	0	11
21	648.9791	6	–1	3	4	44	1360.2373	9	–1	4	5
22	704.2158	7	–5	1	6	45	1394.8143	7	7	7	0
23	742.0761	5	5	5	0						

level of approximation in quantum calculations where the coupled states (CS) approximation might be used instead of the exact close coupling (CC) method. Additional errors might be introduced in rate coefficients if the kinetic energy grid is not fine enough near thresholds, resulting in poor low temperature rate coefficients, or not extended to high enough energies, leading to wrong high temperature results.

Our quantum calculations are carried out with modified versions of the sequential and parallel versions of the MOLSCAT code (Hutson & Green 1994; McBane 2004). Parameters of the propagation are optimized as was done in Dubernet & Grosjean (2002); Grosjean et al. (2003); Dubernet et al. (2006b). Identically to Dubernet et al. (2006b), the H_2 energy levels are the experimental energies of Dabrowski (1984) and the H_2O energy levels and eigenfunctions are obtained by diagonalisation of the effective hamiltonian of Kyrö (1981), compatible with the symmetries of the PES (Dubernet & Grosjean 2002; Grosjean et al. 2003; Dubernet et al. 2006b). The first 45 levels of ortho-water are given in Table 1. The reduced mass of the system is 1.81277373 a.m.u.

2.2.1. Basis set convergence: Methodology in choosing an appropriate basis set

The basis set is a direct product of rotational wavefunctions of water, characterized by the rotational quantum number j_1 (the lowest value of j_1 is one for o-H_2O) and the pseudo-quantum number τ_1 which varies between $-j_1$ and j_1 (alternatively, we may use the pseudo-quantum numbers k_a and k_c with the correspondance $\tau_1 = k_a - k_c$), and of rotational wavefunctions of hydrogen characterised by the rotational quantum number j_2. To a single j_1 rotational quantum number is associated a ladder of increasing rotational energy levels corresponding to successive values of τ_1 characteristic of o-H_2O, and it should be remembered that 2 to 3 adjacent ladders might overlap. A ladder includes j_1 values of τ_1 for even j_1, and j_1+2 values of τ_1 for odd j_1. CC calculations are carried out at a given total energy, a given parity and a total angular momentum J_{tot}. The coupling scheme involves a first coupling between the monomers leading to an intermediate quantum number j_{12}, such that $\hat{j}_{12} = \hat{j}_1 + \hat{j}_2$, and a subsequent coupling to the orbital angular momentum $\hat{l}$ such that $\hat{J}_{tot} = \hat{l} + \hat{j}_{12}$. We call $B(n,m)$ a basis set where n is the maximum value of j_1, m is the maximum value of j_2, and $B(n,m)$ includes all the coupled $|j_{12}, j_1, \tau_1, j_2>$ states. The convergence of the basis set usually involves keeping a number of closed channels above the total energy at which the collisional cross-sections are calculated. These closed channels mainly influence the collisional process in the strong interaction region via coupling of the potential. The potential couplings between $(j_1 k_a k_c)$ energy levels decrease with increasing Δj_1 and Δk_a, therefore for the simple case of a $B(n,0)$ basis set we find that a good convergence is reached with 10 energetically closed channels of water. The basis set $B(n,0)$ with an energy cut-off above the 10th closed channel of water is called a $B^*(n,0)$ [10] basis set (see notation below). Another important question is the accuracy of cross-sections with respect to the number of closed channels of the H_2 molecule. Phillips et al. (1996); Dubernet & Grosjean (2002) already showed that the $j_2 = 2$ level has a strong influence on inelastic cross-sections involving no energy transfer in H_2. Therefore these authors chose basis sets of the type $B(n,2)$, while Grosjean et al. (2003) used a $B(n,3)$ basis set. Generally at least one to two closed H_2 rotational channels would be required in order to ensure convergence to better than 5% of inelactic cross sections involving energy transfer in H_2. This would be particularly important if the purpose of our calculations was to find inelastic rate coefficients of H_2 averaged over water transitions. However for our purposes it is sufficient to use a basis set which is reduced by the application of an energy cut-off, following Dubernet et al. (2006b). We define $B^*(n,m)[p,q,r]$ to be a subset of $B^*(n,m)$ containing, for $j_2 = 0, 2, 4$ respectively, all states of $B^*(n,m)$ up to the first p, q and r states whose internal energies lie above the sum of the total energy and $E(|j_2>)$, where the total energy is taken respective to the ground state of water and p-H_2.

Table 2. Rotational (de)excitation cross-sections (in Å^2) of o-H_2O calculated with different basis sets: (1) a complete $B(6,2)$ basis set, (2) a B*(6,4)[all, all, 5] basis set with an incomplete ladder in $j_2 = 4$, (3) a B*(9,4)[10, 10, 5] basis set with incomplete ladders for $j_2 = 0, 2, 4$. The transitions are labelled by the quantum numbers $j_1 k_a k_c \rightarrow j'_1 k'_a k'_c$ (j_2-j'_2) where primes are final states.

Total energy (cm^{-1})	Transition	B(6,2)	B*(6,4)[all, all, 5]	B*(9,4)[10, 10, 5]	Difference
429.5	$1_{01} \rightarrow 1_{10}$ (0–2)	0.021	0.025		16%
	$1_{01} \rightarrow 1_{10}$ (0–0)	3.890	3.856		0,8%
	$3_{30} \rightarrow 1_{10}$ (0–2)	0.443	0.500		11%
	$3_{30} \rightarrow 1_{10}$ (0–0)	0.106	0.102		4%
681.1	$1_{01} \rightarrow 1_{10}$ (0–2)		0.176	0.175	0.5%
	$1_{01} \rightarrow 1_{10}$ (0–0)		4.3480	4.3489	0.02%
	$3_{30} \rightarrow 1_{10}$ (0–2)		0.9760	0.9773	0.1%
	$3_{30} \rightarrow 1_{10}$ (0–0)		0.1488	0.1481	0.4%
834.9	$1_{01} \rightarrow 1_{10}$ (0–2)	0.268	0.318		16%
	$1_{01} \rightarrow 1_{10}$ (0–0)	4.454	4.412		1%
	$3_{30} \rightarrow 1_{10}$ (0–2)	0.919	0.980		6%
	$3_{30} \rightarrow 1_{10}$ (0–0)	0.194	0.186		4%

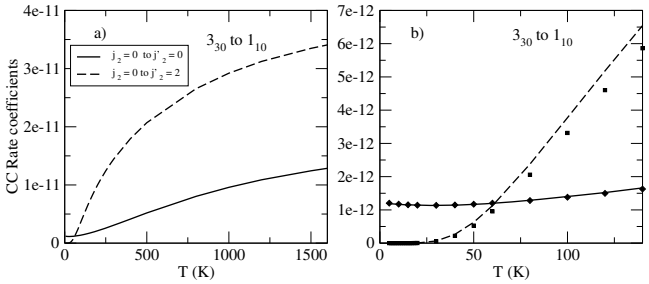

Fig. 1. State-to-state rate coefficients (cm^3 s^{-1}) of the 3_{30} to 1_{10} transition of o-H_2O as a function of temperature (Kelvin). The full line indicates the state-to-state rate coefficients for $\Delta j_2 = 0$, and the broken line corresponds to $\Delta j_2 = 2$. The lines in parts **a)** and **b)** are calculated with a B*(6, 4)[all, all, 5] basis set. Part **b)** also shows rate coefficients obtained with a B(6, 2) basis set (squares and diamonds) at low temperature.

Some behaviors of cross-sections for different basis sets and low lying levels of o-H_2O are shown in Table 2; they are representative of the whole set of cross-sections. At total energy $E_{tot} = 681.1$ cm^{-1}, these cross-sections show less than 0.5% difference between $B^*(6,4)$[all, all, 5] and $B^*(9,4)[10,10,5]$, which includes the open channel 7_{07} and closed channels involving incomplete ladders up to a maximum value of j_1 equal to 9. This result could be considered as trivial but it clearly shows that the convergence procedure of readjusting the number of closed channels for each total energy is solely necessary for total energies covering the opening of molecular channels whose transitions we are interested in; above the highest threshold of interest the basis set does not need to be increased.

Another question is the accuracy of cross-sections with respect to the inclusion of the $j_2 = 4$ level in the basis sets. Table 2 shows that $j_2 = 4$ has the strongest effect on transitions from $j_2 = 0$ to $j_2 = 2$. Overall the inclusion of the $j_2 = 4$ level induces an effect of about 10% to 20% on the strongest state-to-state rate coefficients involving energy transfer in H_2, i.e. for $R(j_1\tau_1 ; j_2 = 0, 2 \rightarrow j'_1\tau'_1 ; j'_2 = 2, 0)(T)$ (and up to 60% for the weakest). This effect is directly transfered to the effective (de)-excitation rate coefficients when they are dominated by those state-to-state rate coefficients. This happens when there is internal energy transfer between excitation of H_2 and de-excitation of o-H_2O. This is illustrated in Fig. 1 for the water transition 3_{30} to 1_{10} where $R(j_1 = 3\,\tau_1 = 3\,j_2 = 2 \rightarrow j'_1 = 1\,\tau'_1 = -1\,j'_2 = 0)(T)$ is larger than $R(j_1 = 3\,\tau_1 = 3\,j_2 = 0 \rightarrow j'_1 = 1\,\tau'_1 = -1\,j'_2 = 0)(T)$.

2.2.2. Basis set convergence: choice of basis set

It is not possible to obtain the same fully converged rate coefficients for all transitions among the first 45 levels of o-H_2O. Therefore we adopted different strategies. For transitions among the first 20 levels of o-H_2O, we adopted one closed channel for H_2 with a maximum value of j_2 equal to 4. For H_2O the basis set combined at least one closed j_1 level and a cut-off in rotational energy equivalent to 10 rotational levels for $j_2 = 0, 2$ (reduced to 5 closed rotational levels for $j_2 = 4$) above the total energy considered in the calculations, i.e. a $B^*(n,4)[10,10,5]$ basis set. This method was employed over the whole range of energies for the de-excitation of the first 10 levels while for de-excitation from the 11th to the 20th levels of o-H_2O it was employed up to a total energy of 950 cm^{-1} only. Due to prohibitive computing cost for total energies from 950 cm^{-1} up to 8000 cm^{-1}, the reduced basis set $B^*(n,2)[10,10]$ was used for de-excitation calculations from the 11th to the 45th levels of o-H_2O with p-H_2.

2.2.3. Choice of method

CC calculations give exact results but are computationally very expensive when they are associated with very large basis sets. Usually CS calculations are prefered for calculations at total energies located far enough from the transition thresholds; therefore the CS method cannot adequately describe collisional de-excitation among the lowest 45 levels of water for total energies up to 2000 cm^{-1}. Moreover we find that the CS method degrades the quality of rate coefficients involving excited rotational levels of H_2 with and without energy transfer in H_2. For non negligeable rate coefficients the errors range from 50% to 100%.

Table 3. Summary of the sets of state-to-state (STSR) $R(j'_1\tau'_1 j'_2 \rightarrow j_1\tau_1 j_2)(T)$ and effective rate coefficients (ER) $\hat{R}_{j_2}(j_1\tau_1 \rightarrow j'_1\tau'_1)(T)$ available in BASECOL. Column 1 labels the set of state-to-state rate coefficients. $T_{\rm min}$(K) and $T_{\rm max}$(K) indicate the lowest and highest temperatures at which calculations and fits have been performed for the relevant sets of data. The column "Transition" indicates the number of levels among which rate coefficients are provided. T1, T2, T3, T4 indicate the expected accuracy: T1 for the 20 first levels of o-H_2O, T2 from the 21st to the 30th level, T3 from the 31st to the 40th, T4 from the 41st to the 45th. A1 means "20% at most for the most significant rates, i.e. larger than 10^{-14}", A2 means "not good but contribute only 4% to effective rate coefficients", the notation $X(Z)Y$ means X% accuracy below a temperature of $T = Z$ Kelvin and Y% accuracy above $T = Z$ Kelvin.

Set				$T_{\rm min}$(K)	$T_{\rm max}$ (K)	Transitions	T1	T2	T3	T4
(1)	$j_2 = 0$	$j'_2 = 0$	STSR	5	1500	45 levels	5%	10%	20(100)10	50(100)10
(2)		$j'_2 = 2$	STSR	5	1500	45 levels	A1			
		$j'_2 = 4$	STSR	–	–	none				
		$\sum_{j'2}$	ER	5	1500	45 levels	5%	15%	20(100)15	50(100)15
(3)	$j_2 = 2$	$j'_2 = 0$	STSR	5	1500	45 levels	A1			
(4)		$j'_2 = 2$	STSR	5	1500	45 levels	10%	25(10)15	40(10)20	50–100(300)25
(5)		$j'_2 = 4$	STSR	1000	1500	10 levels	A2			
		$\sum_{j'2}$	ER	5	1500	45 levels	10%	25(10)15	40(10)20	50–100(300)25
	$j_2 = 4$	$j'_2 = 0$	STSR	–	–	none				
(6)		$j'_2 = 2$	STSR	1000	1500	10 levels	A2			
(7)		$j'_2 = 4$	STSR	5	1500	10 levels	40%			
		$\sum_{j'2}$	ER	5	1500	10 levels	40%			

Therefore our choice was to use the close coupling method over the whole range of total energies.

The failure of the CS method has already been observed by Kouri et al. (1976) for diatom-diatom collisions in the case of HCl-H_2 (Table XI) for transitions that are dominated by the strong long range interaction ($j_2 = 1, 2$). Heil et al. (1978) suggested that the breakdown of the CS approximation is initiated in the short range part of the PES and that the long range anisotropy increases this breakdown. However they assumed that CC and CS would agree better at higher energies. Obviously this is not the case for the present system. It should be noted that even for atom-diatom collisions, Dubernet et al. (2001) showed that CC and CS total inelastic cross-sections among the lowest rotational levels of H_2 colliding with He did not converge at high temperature, though the results were close. In fact, the CS method involves approximating angular momentum terms in the total Hamiltonian, and in particular omitting Coriolis terms. When the angular momentum of the hydrogen molecule is introduced into the problem, the validity of these approximations for the angular momentum coupling is likely to be compromised. The large energy spacing of the rotational levels of hydrogen will exacerbate these effects.

2.2.4. Choice of total energy points

CC calculations are carried out over essentially the whole energy range spanned by the Boltzmann distributions (Eq. (1)); the highest energy point calculated is at 8000 cm^{-1} and cross sections are extrapolated at higher energy in order to achieve convergence for de-excitation from the highest water energy levels. These extrapolations do not degrade the accuracy of rate coefficients because the concerned cross sections behave regularly. We carefully spanned the energy range above the inelastic channels and added more points in the presence of resonance structures. The total energy grid below the 10th threshold has been described in Dubernet et al. (2006b); between the 10th and the 20th threshold energy steps vary from 0.5 to 2 cm^{-1}, from the 20th to the 25th they range from 2 to 5 cm^{-1}, above the 25th threshold they vary from 10 to 40 cm^{-1}. We paid particular attention to having a fine description of low energy behaviors of cross sections connected to $j_2 = 2$ for rotational levels of H_2O up to 600 cm^{-1}. Nevertheless for $j_2 = 2$ the energy grid is coarser than for $j_2 = 0$, though still allowing an adequate precision (see Table 3). Overall there are about 1592 energy points.

3. Discussion

3.1. Results for $j_2 = 0, 2, 4, 6, 8$

We use the methodology described above to calculate sets of state-to-state rate coefficients (Eq. (1)) in the temperature range from 5 K to 1500 K for de-excitation transitions among the 45 lowest levels of o-H_2O with $j_2 = 0$ and $\Delta j_2 = 0, +2$, as well as with $j_2 = 2$ and $\Delta j_2 = 0, -2$. In addition and only for the 10 lowest energy levels of o-H_2O, we obtain cross sections involving $j_2 = 4$ with $\Delta j_2 = 0, -2, -4$, $j_2 = 0$ with $\Delta j_2 = 0, +2, +4$ and $j_2 = 2$ with $\Delta j_2 = 0, +2, -2$. Because of the sparse energy grid of cross sections involving $j_2 = 4$, we estimate that the related rate coefficients are only correct for temperatures above 1000 K. All rate coefficients involving energy transfers with $\Delta j_2 = \pm 4$ are very small and can be ignored up to 1500 K. The state-to-state rate coefficients involving energy transfers from $j_2 = 2$ to $j_2 = 4$ or from $j_2 = 4$ to $j_2 = 2$ contribute only 4% to the effective rate coefficients; nevertheless we provide them for the sake of completeness between 1000 K and 1500 K. They should only be used to calculate the effective excitation and de-excitation rate coefficients of o-H_2O out of the $j_2 = 2, 4$ level as their accuracy is quite low.

Additionally we use the breathing sphere approximation (Agg & Clary 1991a,b), i.e. we average the PES over $j_2 = 4$ in order to complete the set of de-excitation cross sections of o-H_2O with $j_2 = 4$ and $\Delta j_2 = 0$, which allows us to obtain rate coefficients for temperatures between 5 K and 1500 K. This procedure is fully justified by the small magnitude of cross sections involving energy transfer with $\Delta j_2 = -2, -4$ from $j_2 = 4$.

From the calculated state-to-state rate coefficients, the effective rate coefficients corresponding to $j_2 = 0, 2, 4$ can be calculated using Eq. (3). The ratios of effective de-excitation rate coefficients (Eq. (3)) $\hat{R}_{j_2=2}$ ($\hat{R}_{j_2=4}$) over effective de-excitation rate coefficients $\hat{R}_{j_2=0}$ ($\hat{R}_{j_2=2}$) for the first 45 (10) levels of ortho-water are given in Figs. 2, 3. Table 4 provides the correspondance between labels of the 990 transitions and labels of the energy levels given in Table 1.

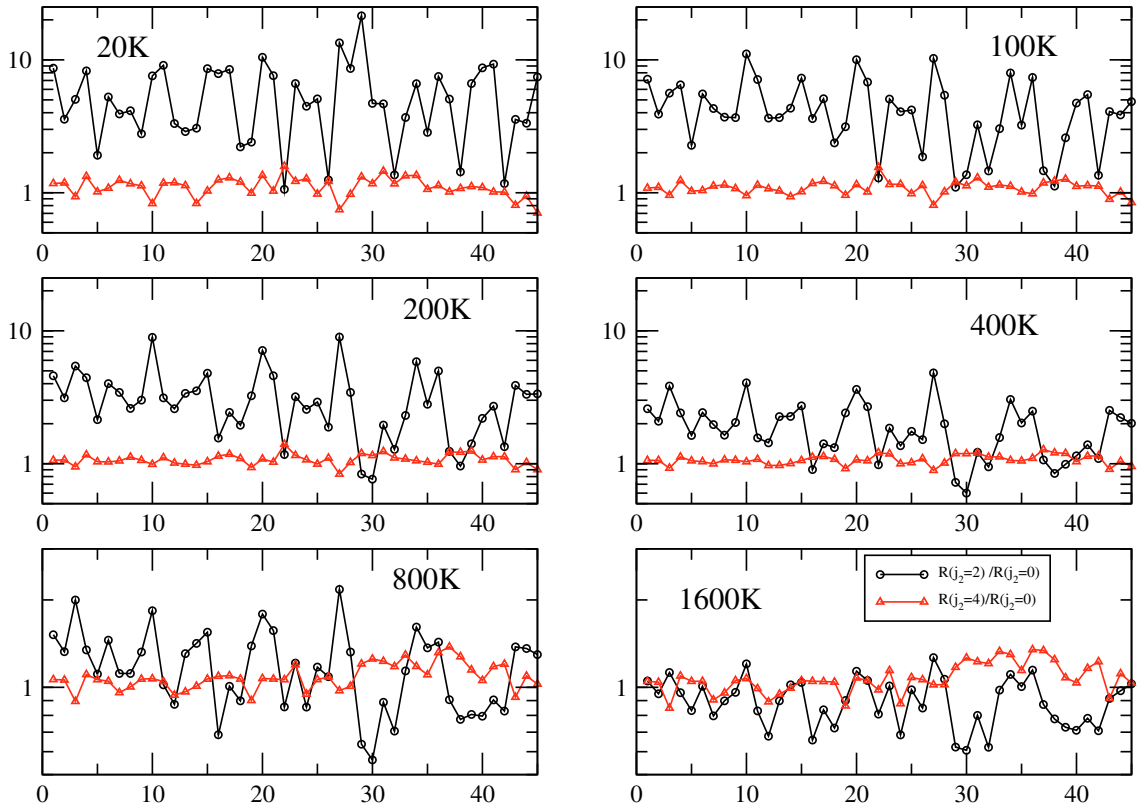

Fig. 2. Ratios of effective de-excitation rate coefficients (Eq. (3)) for the first 10 levels of o-water and for temperatures ranging from 20 K to 1600 K. Black lines give the ratios $\hat{R}_{j_2=2}/\hat{R}_{j_2=0}$ and red lines give the ratios $\hat{R}_{j_2=4}/\hat{R}_{j_2=2}$. The abscissae indicate the labeling of the de-excitation transitions as indicated in Table 4.

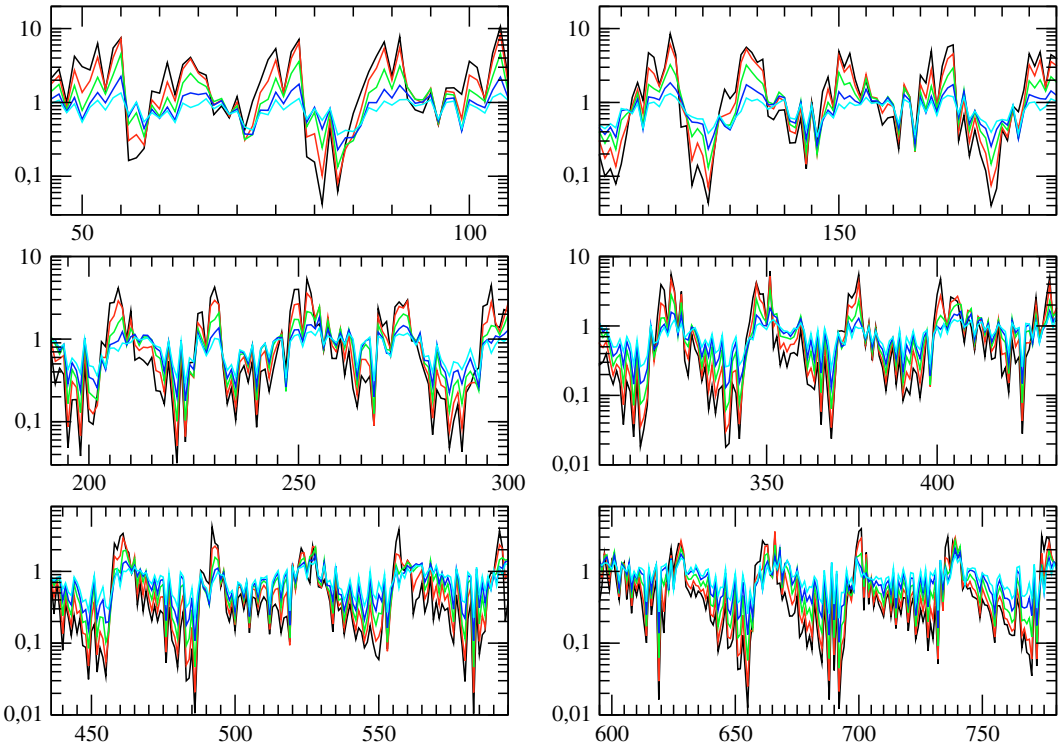

Fig. 3. Ratios of effective de-excitation rate coefficients (Eq. (3)) $\hat{R}_{j_2=2}/\hat{R}_{j_2=0}$ from the 46th to the 990th de-excitation transition and for the following temperatures: T = 100 K (black), T = 200 K (red), T = 400 K (green), T = 800 K (blue), T = 1600 K (cyan). The abscissae indicate the labeling of the de-excitation transitions as indicated in Table 4.

Table 4. Labels of first and last de-excitation transitions from a given level (as given in Table 1). This table is the key for reading the figures giving ratios of rate coefficients as a function of transitions labels.

Level	First	Last	Level	First	Last	Level	First	Last
2	1	1	17	121	136	32	466	496
3	2	3	18	137	153	33	497	528
4	4	6	19	154	171	34	529	561
5	7	10	20	172	190	35	562	595
6	11	15	21	191	210	36	596	630
7	16	21	22	211	231	37	631	666
8	22	28	23	232	253	38	667	703
9	29	36	24	254	276	39	704	741
10	37	45	25	277	300	40	742	780
11	46	55	26	301	325	41	781	820
12	56	66	27	325	351	42	821	861
13	67	78	28	352	378	43	862	903
14	79	91	29	379	406	44	904	946
15	92	105	30	407	435	45	947	990
16	106	120	31	436	465			

Ratios $\hat{R}_{j_2=2}/\hat{R}_{j_2=0}$ can be very large for water transitions for which no internal energy transfer occurs between H_2 and H_2O; these large ratios are due to the strong long range part of the PES for $j_2 = 2$. These ratios can as well be very small when internal energy transfer strongly enhances $\hat{R}_{j_2=0}$ rate coefficients. The alternating large and small ratios lead to the patterns observed in Fig. 3; these patterns are particularly noticeable for de-excitation from high lying energy levels of water. Indeed $\hat{R}_{j_2=0}(\alpha \rightarrow \alpha')$ de-excitation effective rate coefficients are strongly influenced by the corresponding state-to-state rate coefficients $R(j_2 = 0 \rightarrow j_2' = 2; \alpha \rightarrow \alpha')$ for all o-water α levels above the opening of the $j_2 = 2$ level of H_2, while $\hat{R}_{j_2=2}(\alpha \rightarrow \alpha')$, $\hat{R}_{j_2=4}(\alpha \rightarrow \alpha')$ effective rate coefficients are mainly influenced by respectively the $R(j_2 = 2 \rightarrow j_2' = 2; \alpha \rightarrow \alpha')$ and $R(j_2 = 4 \rightarrow j_2' = 4; \alpha \rightarrow \alpha')$ state-to-state rate coefficients.

Effective rate coefficients of o-H_2O linked to $j_2 = 6, 8$ may also be obtained using the breathing sphere approximation between 5 K and 1500 K. Indeed Dubernet et al. (2001) (in Fig. 2) showed that total inelastic cross-sections of H_2 with $j_2 = 4$, 6 colliding with He are negligeable in the energy range from 0 cm^{-1} to 5000 cm^{-1} and we can assume a similar behavior in the present case. Nevertheless this work is not performed in the present paper and the magnitudes of the relevant effective rate coefficients may be evaluated using multiplicative factors with the following guideline, based on available comparisons among our calculated rate coefficients between $j_2 = 2$ and $j_2 = 4$: the user may vary the effective rate coefficient by 20%–50% (mostly increase) from $j_2 = 2$ to $j_2 = 4$, and so on up to $j_2 = 8$.

The BASECOL database (Dubernet et al. 2006a) will provide full tables of the rate coefficients sets mentioned in Table 3.

3.2. Accuracy of results

Apart from the usual checks of convergence with respect to propagation parameters, basis set and total angular momentum, the state-to-state rate coefficients have been carefully checked by detailed balance. It should be recalled that the quality of rate coefficients at low temperature is linked to the number of energy points close to the molecular thresholds, and we have an excellent energy grid for $j_2 = 0$ and a sparser but still good energy grid for $j_2 = 2$. We have a very good grid for $j_2 = 4$, due to the use of the breathing sphere approximation at total energy close to water thresholds. The maximum values of the estimated errors are given in Table 3 for transitions starting from different levels of o-H_2O (T1, T2, T2, T4) and for the various sets of state-to-state rate coefficients (1 to 7). Sets (5) and (6) have very low accuracy, which is not a cause for concern for the present application since they provide a very small contribution to the effective rate coefficients. The accuracy of the effective rate coefficients (ER) $\hat{R}_{j_2=0}$ reflects the accuracies of set (1) and of set (2) to a lesser extent. The accuracy of the effective rate coefficients (ER) $\hat{R}_{j_2=2}$ is mainly connected to set (4) because set (3) rate coefficients give a small contribution to the effective rate coefficients. The accuracy of the effective rate coefficients linked to $j_2 = 4$ can be estimated to be around 40%.

3.3. Thermalized rate coefficients

We will not explicitly provide de-excitation rate coefficients of o-H_2O with thermalized H_2 (Eq. (4)). The values of $g_{j_2} e^{-\frac{E_{\rm int}(H_2)}{k_B T}}$ in Table 5 indicate that we can provide accurate averaged de-excitation rate coefficients (Eq. (4)) up to 300 K–400 K for transitions from the 11th–45th level of o-H_2O, and up to 800 K for the 10 first levels, the accuracy being that of the state-to-state rate coefficients. When levels $j_2 > 2$ start to contribute to thermalised rate coefficients, the uncalculated effective rate coefficients for $j_2 > 2$ might be estimated using the guidelines given in Sect. 3.1. Another possibility at high temperature is to directly use the QCT rate coefficients of Faure et al. (2007), being aware of their limitation. Extensive comparisons between our averaged de-excitation rate coefficients and the QCT results are given in the following sections.

3.4. Overestimation of rate coefficients by QCT calculations

The calculations of Faure et al. (2007) are described in the introduction. At 20 K a comparison between the present results and the Faure et al. (2007) results only indicates whether those authors were right to claim that their linear extrapolation from 100 K lies within a factor of 2 to 3 of the true values. In order to compare quantum and QCT results obtained with the same PES, we must remove the scaled H_2O-He results from their published set since the scaled H_2O-He rate coefficients are used for 65% of the transitions at various temperatures. Figure 4 shows the ratios of averaged CC rate coefficients over thermalized QCT rate coefficients for temperatures 100 K, 200 K, 800 K and 1600 K (note that averaged CC rate coefficients involve $j_2 = 0, 2, 4$ for

Table 5. Unnormalized population of the rotational states of p-H_2 relative to $j_2 = 0$, at different temperatures and assuming thermodynamic equilibrium.

j_2 / T(K)	10	100	140	200	400	600	800	1200	1500
0	1	1	1	1	1	1	1	1	1
2	–	0.028	0.122	0.37	1.36	2.1	2.6	3.24	3.54
4	–	–	–	–	0.12	0.5	1.0	2.13	2.84
6	–	–	–	–	–	0.03	0.14	0.63	1.15
8	–	–	–	–	–	–	–	0.09	0.27

Table 6. Quantum numbers of levels involved in the transitions of Fig. 5 **a)**, **b)**, **c)** overestimated by QCT calculations. Primes indicate quantum numbers of the final states.

Transitions	j	τ	k_a	k_c	j'	τ'	k'_a	k'_c
71	5	–3	1	4	3	–3	0	3
74					4	–3	1	4
77					5	–5	0	5
221	7	–5	1	6	5	–5	0	5
225					6	–5	1	6
229					7	–7	0	7
580	9	–7	1	8	7	–7	0	7
585					8	–7	1	8
591					9	–9	0	9

transitions among the first 10 levels of water and $j_2 = 0, 2$ for all other transitions). We find that the QCT method systematically overestimates, by up to a factor of 10, some of the strongest rate coefficients and underestimates rate coefficients involving internal energy transfer between o-H_2O and H_2 by factors as large as 100 at T = 100 K. The agreement between the two sets of rate coefficients improves with increasing temperature and above T = 800 K most rates are within a factor of 3.

The overestimation of some of the strongest thermalized rate coefficients concerns a few transitions over the whole range of temperature. This effect is not related to the missing $j_2 = 4$ quantum effective rate coefficient since the overestimation exists for temperatures below 400 K. Figure 5 compares our CC averaged rate coefficients with the set published by Faure et al. (2007) and with scaled He rate coefficients of Green et al. (1993) for transitions from the 5_{14}, 7_{16}, 9_{18}, 6_{25} levels. These last 2 sets coincide for some transitions since Faure et al. (2007)'s set includes both QCT calculations and scaled He rate coefficients for the weakest transitions. QCT calculations systematically overestimate transitions from the 5_{14}, 7_{16}, 9_{18} levels to the lowest level of a j ladder (indicated by arrows), with the strongest overestimation corresponding to a transition in the same ladder (bold arrows). Table 6 gives the initial and final quantum numbers of the involved transitions. These overestimations seem to exist for initial j having odd values only. Indeed for even j no such overestimation is observed, as can be seen in part (d) of Fig. 5 for de-excitation from the 6_{25} level. We suspect that these systematic overestimations are an artefact of the binning procedure in the QCT calculations of Faure et al. (2007).

3.5. Underestimation of rate coefficients by scaled He and QCT calculations

The de-excitation rate coefficients of H_2O + He of Green et al. (1993), scaled by a factor of 1.344 to correct for the differing colliding system masses, have systematically been used in astrophysical applications to mimic rate coefficients of H_2O + H_2. Phillips et al. (1996) had already pointed out that this method was not correct for temperatures up to 140 K. Figures 6, 7 show that scaled H_2O + He rate coefficients underestimate both the $j_2 = 0$ effective and thermalized rate coefficients, with ratios as large as 1000. The largest ratios occur for transitions dominated by internal energy transfer between H_2 and H_2O. This induces larger rate coefficients for the concerned water transitions and the effect is particularly noticeable for de-excitation from high lying levels of water and for transitions involving favorable quantum numbers, i.e. Δj_1, Δk_a small.

Examples of transitions largely underestimated at 100 K by both scaled He and QCT calculations are given in Table 7. The ratios of CC averaged de-excitation rate coefficients of o-H_2O with p-H_2 over QCT calculations of Faure et al. (2007) are nevertheless smaller than the ratios of CC averaged de-excitation rate coefficients over scaled water-He rate coefficients (Green et al. 1993). Apart from the overestimation cases analyzed above, QCT calculations generally are an improvement over scaled He calculations. It is unfortunate that very few rate coefficients can be calculated via QCT calculations.

Figures 8 to 13 compare our averaged rate coefficients with the set published by Faure et al. (2007) and with scaled He rate coefficients of (Green et al. 1993) for some of the 990 de-excitation transitions from the first 45 levels of ortho-water. Again we recall that these last 2 sets coincide for some transitions since Faure et al. (2007)'s set includes both QCT calculations and scaled He rate coefficients for the weakest transitions.

3.6. Comparison with the H_2O + H_2 effective rate coefficients of Phillips et al. (1996)

Comparison with effective rate coefficients of Phillips et al. (1996) can only be performed for the first 10 levels of o-H_2O and for temperatures in the range 20 K to 140 K. The ratios of effective rate coefficients, given in Table 8, decrease slightly with temperature. This certainly reflects the decreasing influence of the difference between the two different PES (Phillips et al. 1994; Faure et al. 2005a) as temperature increases. The first line of Table 8 shows that the $j_2 = 2$ level cannot be ignored in the calculation of the averaged rate coefficients above T = 120 K.

3.7. Fitted rate coefficients

The state-to-state rate coefficients $R(j_1\tau_1 j_2 \rightarrow j'_1\tau'_1 j'_2)(T)$ for the de-excitation of o-H_2O with p-H_2($j_2 = 0, 2, 4$) and $\Delta j_2 = 0, \pm 2$ are fitted to an analytical form very similar to the one used by Mandy & Martin (1993):

$$\log_{10} R(T) = \sum_{k=1}^{N-1} a_k \left[\log_{10} \frac{T}{\epsilon}\right]^{k-1} + a_N \left(\frac{1}{T/\epsilon + \epsilon} - 1\right). \quad (5)$$

The fits are performed using numerical rate coefficients calculated at ~100 temperatures ranging from T_{min} to T_{max} which

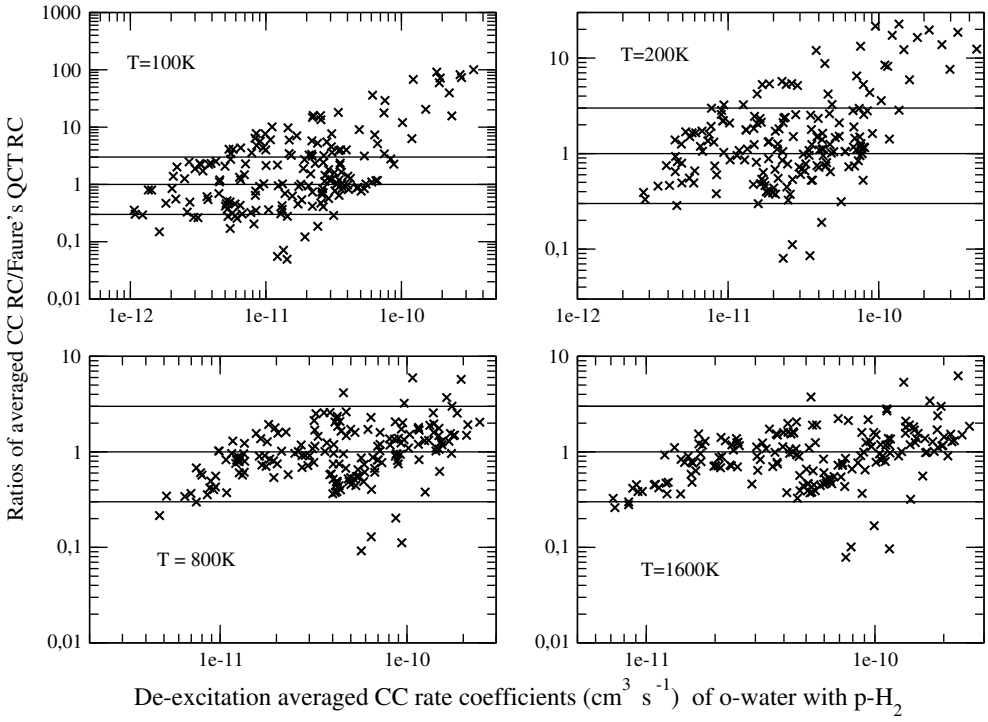

Fig. 4. Ratios of CC averaged de-excitation rate coefficients (Eq. (4)) of o-H_2O with p-H_2 over QCT calculations of Faure et al. (2007) as a function of the CC averaged de-excitation rate coefficients of o-H_2O with p-H_2 (in cm^{3}s^{-1}).

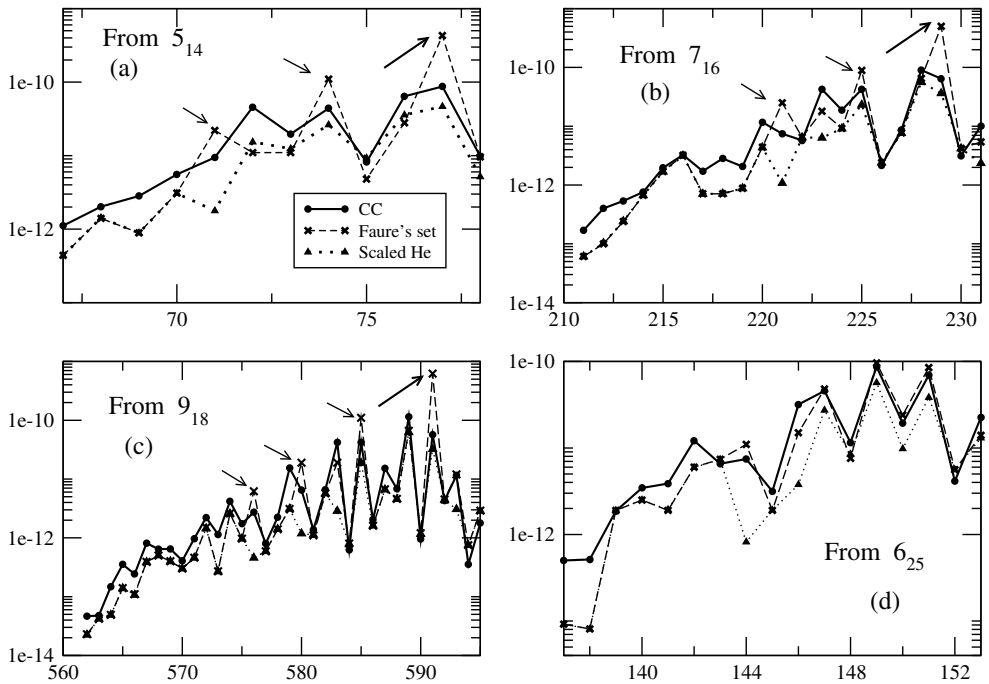

Fig. 5. Comparison of de-excitation rate coefficients (in cm^3 s^{-1}) at T = 800 K from the **a)** 5_{14}, **b)** 7_{16}, **c)** 9_{18} and **d)** 6_{25} levels of o-water. The full lines (with circles) correspond to our CC averaged rate coefficients (Eq. (4) as explained in the text), the dashed lines to the set of de-excitation rate coefficients of Faure et al. (2007), the dotted lines to the scaled He rate coefficients of Green et al. (1993). The abscissae correspond to the index of the transition with quantum numbers indicated in Table 6.

are indicated in Table 3. The fitted coefficients are such that the maximum error between initial data points and fitted values is minimal. A maximum value of N = 14 is necessary in order to obtain good accuracy over the whole range of temperature. The fitted rate coefficients were subsequently compared to numerical rate coefficients calculated with a step of T = 1 K from T_{min} to T_{max} and the maximum error found is less than 0.5%. We emphasize that these fits have no physical meaning; they are only valid in the temperature range of the relevant T_{min}, T_{max} and should not be used to perform extrapolations. The

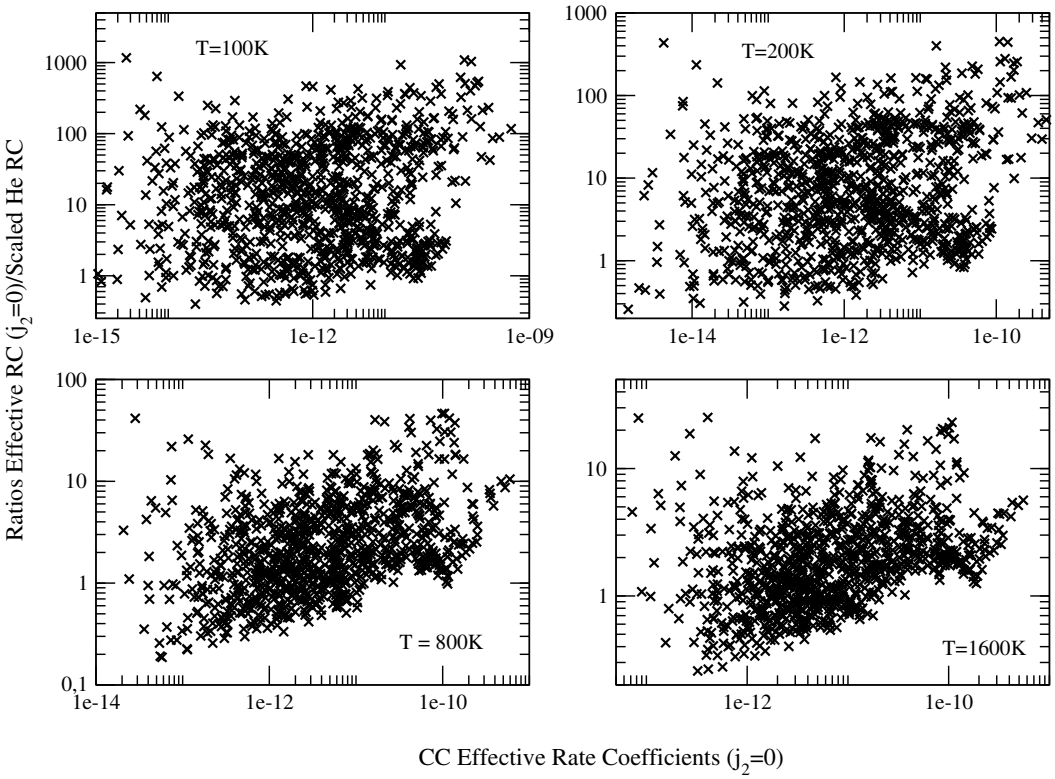

Fig. 6. Ratios of effective de-excitation rate coefficients (Eq. (3)) of o-H_2O with $H_2(j_2 = 0)$ over scaled water-He rate coefficients (in $cm^3\ s^{-1}$) (Green et al. 1993) as a function the CC averaged de-excitation rate coefficients of o-H_2O with p-H_2 (in $cm^3\ s^{-1}$).

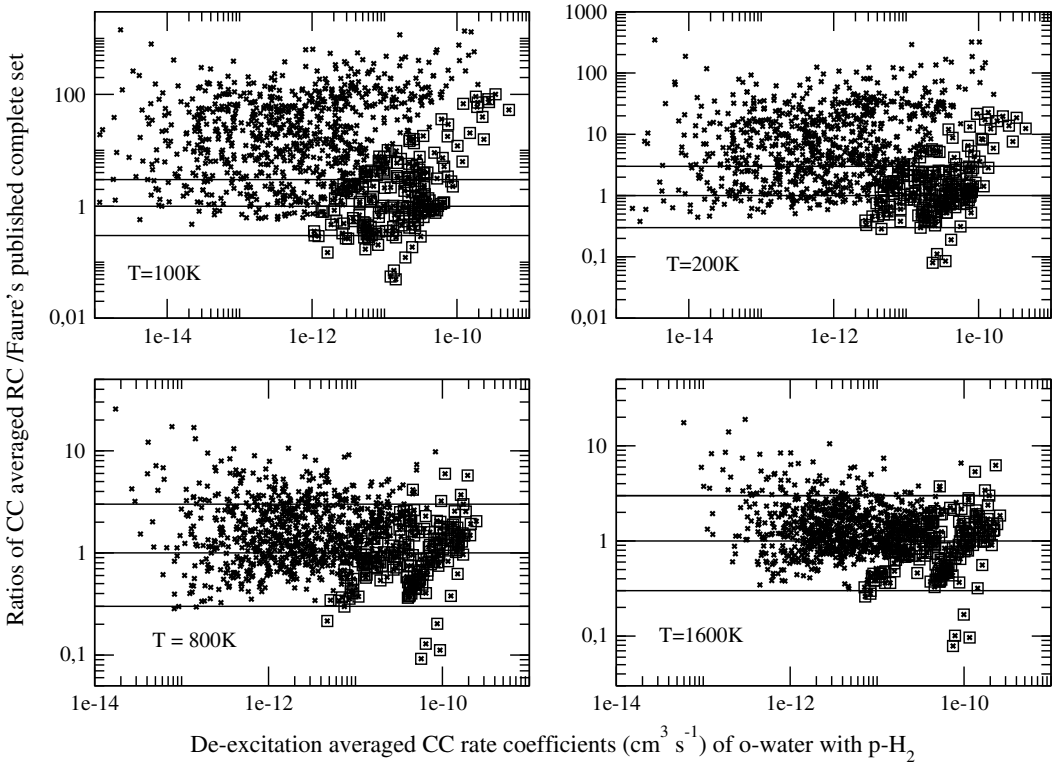

Fig. 7. Ratios of CC averaged de-excitation rate coefficients (Eq. (4)) of o-H_2O with p-H_2 over data sets published by Faure et al. (2007) as a function the CC averaged de-excitation rate coefficients of o-H_2O with p-H_2 (in $cm^3\ s^{-1}$). These data sets include both the quasi-classical calculations (crosses in squares) and scaled water-He rate coefficients (crosses without squares) published in Faure et al. (2007).

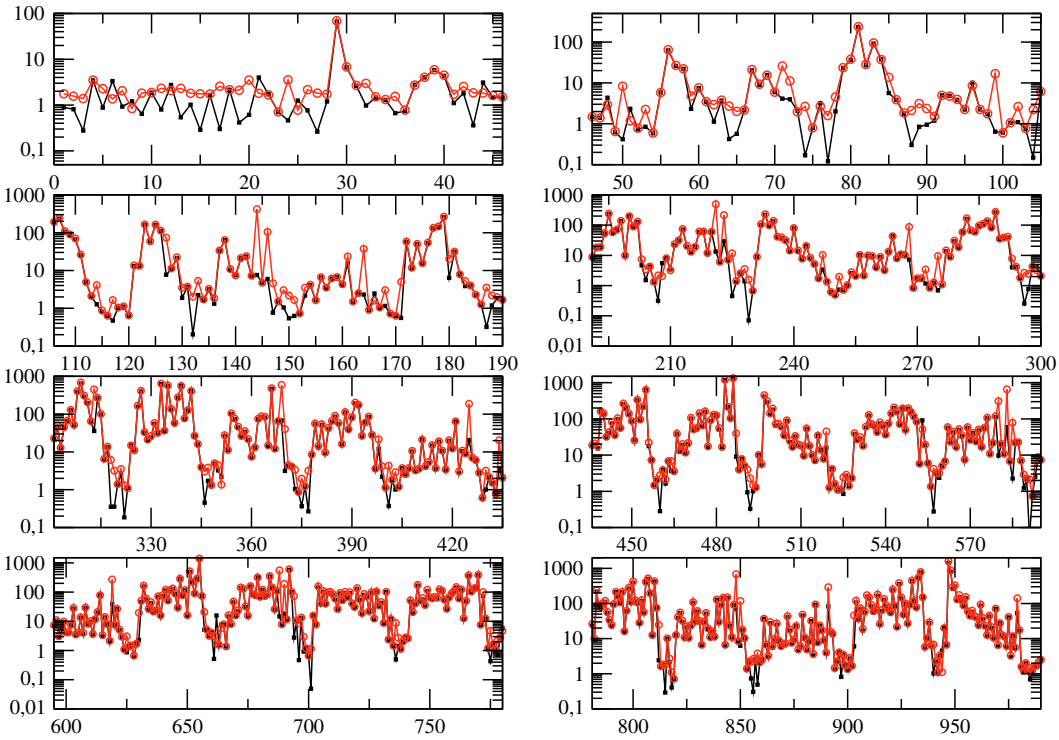

Fig. 8. Ratios of CC averaged de-excitation rate coefficients (Eq. (4)) of o-H_2O with p-H_2 over the set of rate coefficients published by Faure et al. (2007) (black line) and over scaled He rate coefficients of (Green et al. 1993) (red line) for all 990 de-excitation transitions from the first 45 levels of o-water at a temperature of 100 K. The abscissae indicate the labeling of the de-excitation transitions as indicated in Table 4.

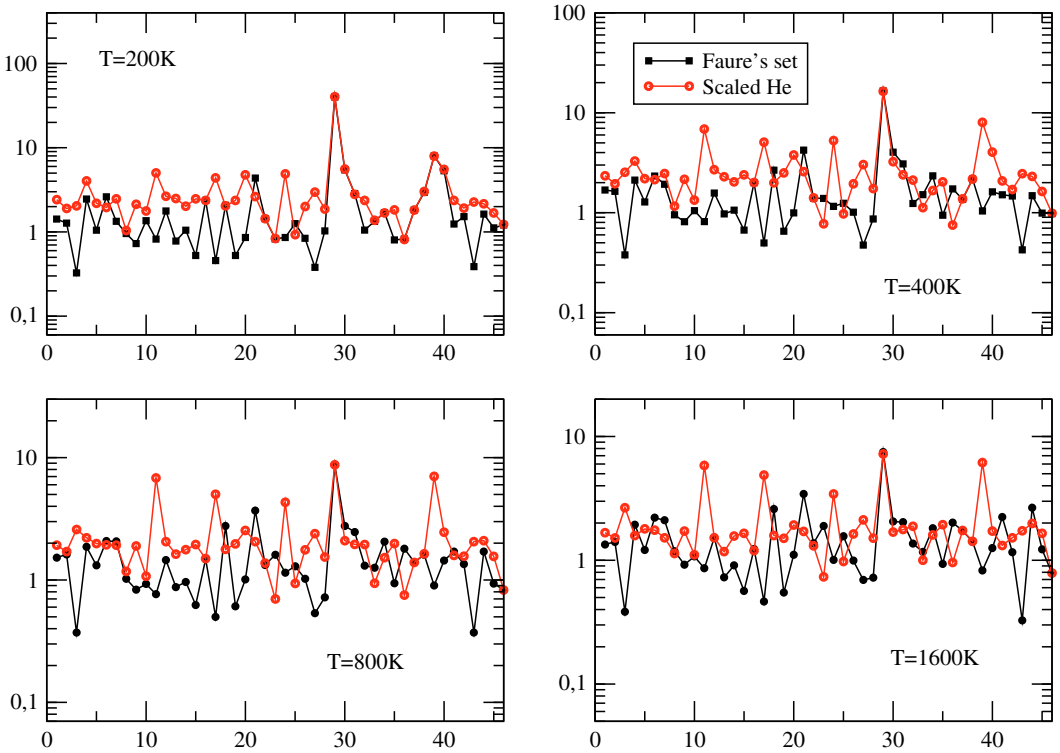

Fig. 9. Ratios of CC averaged de-excitation rate coefficients (Eq. (4)) of o-H_2O with p-H_2 over the set of rate coefficients published by Faure et al. (2007) (black line) and over scaled He rate coefficients of Green et al. (1993) (red line) given for the first 45 de-excitation transitions from the first 10 levels of o-water, for temperatures ranging from 200 K to 1600 K. The abscissae indicate the labeling of the de-excitation transitions as indicated in Table 4.

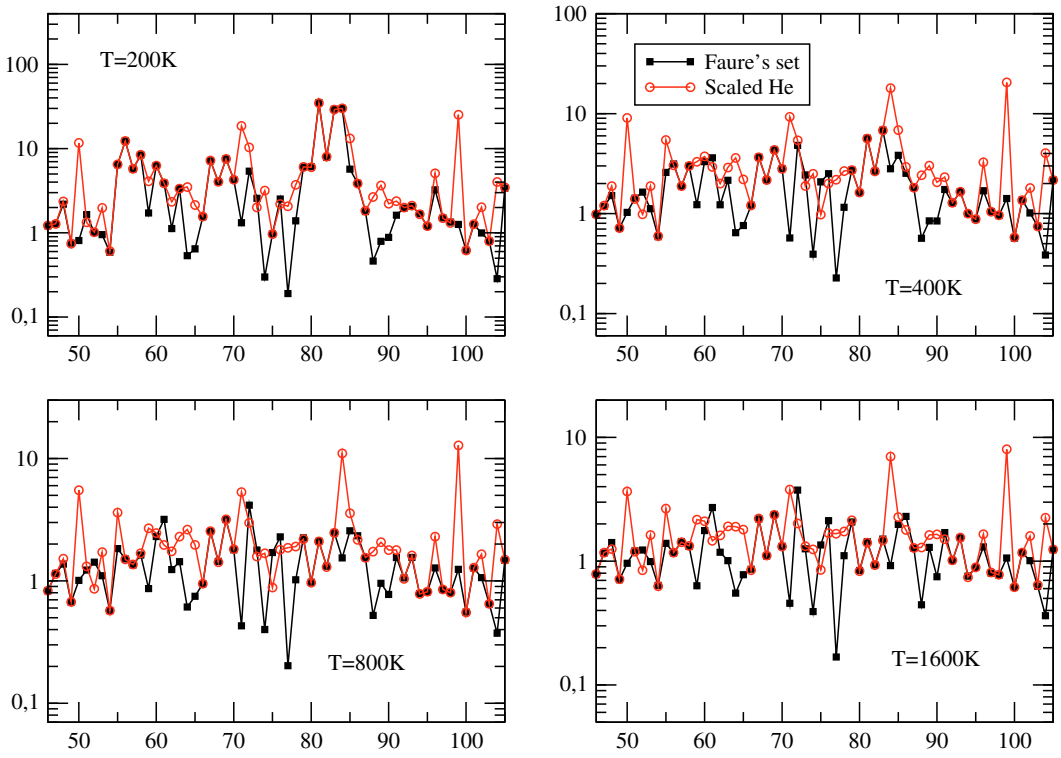

Fig. 10. Ratios of CC averaged de-excitation rate coefficients (Eq. (4)) of o-H_2O with p-H_2 over the set of rate coefficients published by Faure et al. (2007) (black line) and over scaled He rate coefficients of Green et al. (1993) (red line) for the 46th to the 105th de-excitation transitions from the first 15 levels of o-water for temperatures ranging from 200K to 1600 K. The abscissae indicate the labeling of the de-excitation transitions as indicated in Table 4.

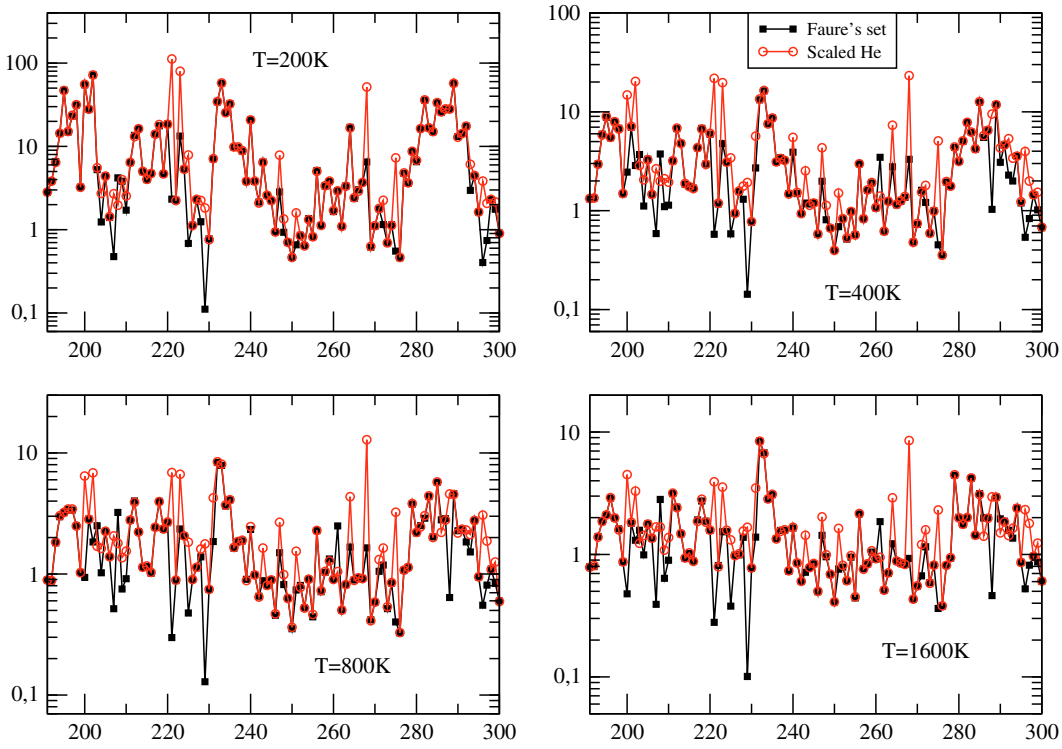

Fig. 11. Ratios of CC averaged de-excitation rate coefficients (Eq. (4)) of o-H_2O with p-H_2 over the set of rate coefficients published by Faure et al. (2007) (black line) and over scaled He rate coefficients of Green et al. (1993) (red line) for the 191st to the 300th de-excitation transitions from the first 25 levels of o-water for temperatures ranging from 200 K to 1600K. The abscissae indicate the labeling of the de-excitation transitions as indicated in Table 4.

Table 7. Levels involved in some of the transitions largely underestimated by scaled He calculations and to a lesser extent by QCT calculations at 100 K. We provide ratios of averaged CC rate coefficients over QCT and scaled He calculations at 100 K, as well as the values of the corresponding averaged CC rate coefficients (in $cm^3\ s^{-1}$).

Transitions	Initial Level	Final Level	CC value	Ratios (CC/QCT)	Ratios (CC/He)
127	17	7	8.5e-12	7	66
144	18	8	9.9e-12	7	68
180	20	9	8.3e-12	7	32
223	22	13	7.5e-11	30	191
268	24	15	6.3e-11	7	55
313	26	13	6.1e-11	36	142
425	30	19	1.5e-10	20	328
456	31	21	7.4e-11	17	15
487	32	22	4.9e-11	9	42
519	33	23	2.3e-10	15	38
553	34	25	1.8e-10	91	45
583	35	22	1.9e-10	59	1800
619	36	24	2.2e-10	39	773
690	38	24	3.4e-11	18	683
732	39	29	3.4e-10	100	142

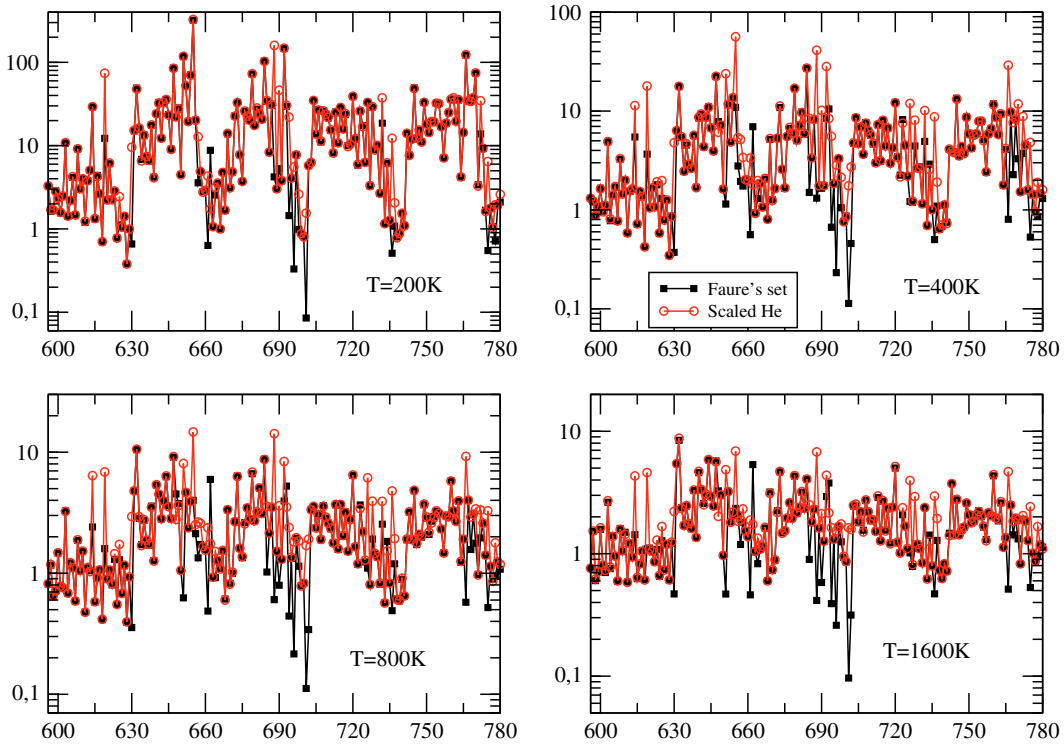

Fig. 12. Ratios of CC averaged de-excitation rate coefficients (Eq. (4)) of o-H_2O with p-H_2 over the set of rate coefficients published by Faure et al. (2007) (black line) and over scaled He rate coefficients of Green et al. (1993) (red line) for the 596th to the 780th de-excitation transitions from the first 35 levels of o-water for temperatures ranging from 200 K to 1600 K. The abscissae indicate the labeling of the de-excitation transitions as indicated in Table 4.

complete sets including levels up to the 45th will be available in the BASECOL database (Dubernet et al. 2006a). The quality of the fits can be checked on line through the graphical interface.

4. Concluding remarks

We provide state-to-state rate coefficients among the 45 lowest levels of o-H_2O with H_2 ($j_2 = 0$) and $\Delta j_2 = 0, +2$, as well as with $j_2 = 2$ and $\Delta j_2 = 0, -2$. In addition and only for the 10 lowest energy levels of o-H_2O, we obtain state-to-state rate coefficients involving $j_2 = 4$ with $\Delta j_2 = 0, -2$ and $j_2 = 2$ with $\Delta j_2 = +2$.

For the given PES the accuracy of quantum rate coefficients, explicitly given for different temperatures and transitions, is rather homogeneous and lies between 5% and 40% for the first 40 levels of o-H_2O. For the available transitions, we strongly recommend use of the present sets of effective rate coefficients instead of either the scaled H_2O-He data of Green et al. (1993) or the set published in Faure et al. (2007). For temperatures above 400 K, thermalized rate coefficients start to include $j_2 > 2$ effective rate coefficients for which we do not provide exact quantum results for all transitions. We advise the user to use multiplicative factors in order to estimate these missing effective rate

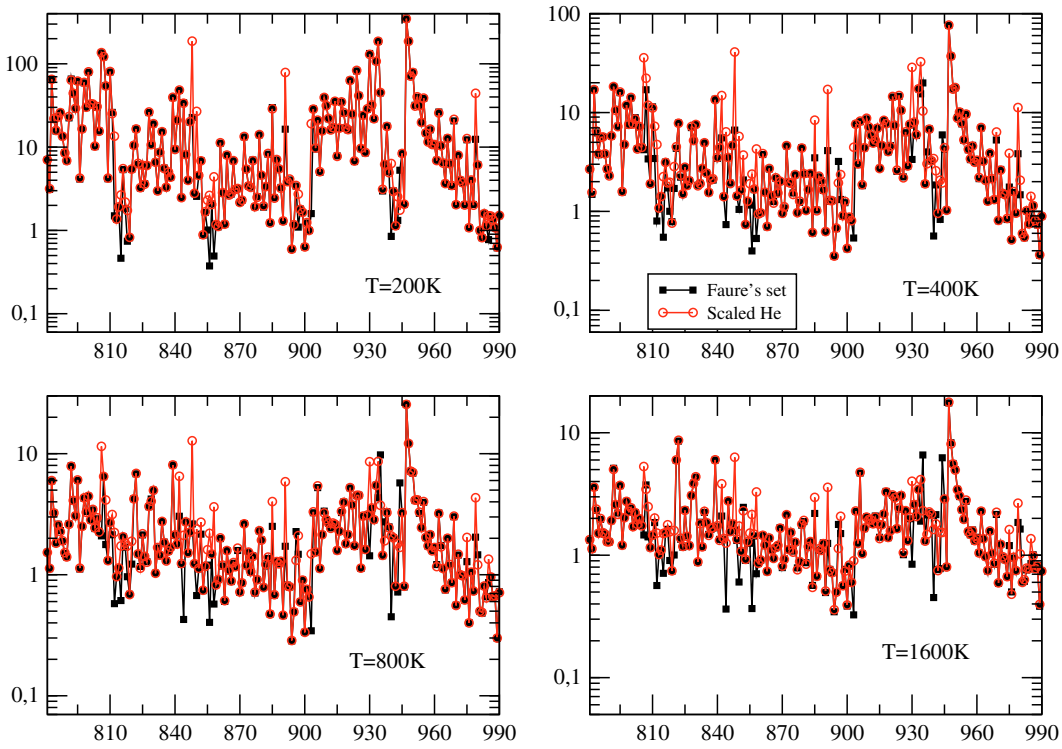

Fig. 13. Ratios of CC averaged de-excitation rate coefficients (Eq. (4)) of o-H_2O with p-H_2 over the set of rate coefficients published by Faure et al. (2007) (black line) and over scaled He rate coefficients of Green et al. (1993) (red line) for the 781st to the 990th de-excitation transitions from the first 35 levels of o-water for temperatures ranging from 200 K to 1600 K. The abscissae indicate the labeling of the de-excitation transitions as indicated in Table 4.

Table 8. Ratios of the 5 effective de-excitation rate coefficients of Phillips et al. (1996) over our averaged rate coefficients (1st line) for o-H_2O with p-H_2. The ratios of Phillips et al.'s results over our effective rate coefficients (Eq. (3)) for $j_2 = 0$ for o-H_2O with para-H_2 are given on every second line.

Transitions/T (K)	20	40	60	80	100	120	140
2 1	2.86	2.09	1.87	1.84	1.97	2.21	2.46
	2.86	2.09	1.86	1.74	1.66	1.62	1.57
3 1	1.68	1.58	1.56	1.57	1.65	1.77	1.93
	1.68	1.58	1.55	1.53	1.52	1.49	1.48
3 2	0.95	0.94	0.91	0.90	0.95	1.06	1.21
	0.95	0.94	0.90	0.86	0.83	0.81	0.79
4 1	0.75	0.78	0.83	0.92	1.08	1.32	1.60
	0.75	0.78	0.83	0.87	0.93	0.99	1.04
4 2	1.59	1.58	1.56	1.56	1.58	1.62	1.70
	1.59	1.58	1.55	1.54	1.52	1.50	1.48
4 3	2.13	2.06	1.99	1.98	2.07	2.27	2.48
	2.13	2.06	1.98	1.90	1.82	1.77	1.71
5 1	0.86	0.88	0.88	0.91	0.98	1.10	1.25
	0.86	0.88	0.88	0.88	0.89	0.90	0.93
5 2	1.60	1.52	1.51	1.53	1.60	1.70	1.82
	1.60	1.52	1.51	1.49	1.48	1.46	1.45
5 3	1.57	1.50	1.50	1.52	1.60	1.72	1.89
	1.57	1.50	1.49	1.49	1.49	1.47	1.47
5 4	1.97	1.69	1.55	1.54	1.73	2.12	2.64
	1.97	1.69	1.54	1.42	1.34	1.27	1.24

coefficients. Above 400 K the user can also choose to use the set published in Faure et al. (2007), being aware that the weakest transitions are given by scaled H_2O-He rate coefficients which are sometimes wrong by large factors. As expected we find that the scaled He rate coefficients (Green et al. 1993) are neither representative of the effective rate coefficients $\hat{R}_{j_2=0}$ nor of the averaged CC rate coefficients.

Finally we find that the CS approximation fares extremely badly even at high energy for j_2 not equal to zero. We will investigate the breakdown of the CS approximation in another publication.

We are currently carrying out similar calculations for o-H_2O with o-H_2 (j_2 = 1, 3) and for p-H_2O with o/p-H_2.

Acknowledgements. Most scattering calculations were performed at the IDRIS-CNRS and CINES under project 2006-07-08 04 1472. This research was supported by the CNRS national program "Physique et Chimie du Milieu Interstellaire" and by the FP6 Research Training Network "Molecular Universe", contract Number: MRTN-CT-2004-512302. The authors thank P. Valiron and A. Faure for critical reading of early drafts and the referee for pertinent remarks. Since the submission of this paper, P. Valiron has passed away and we dedicate this paper to his memory.

References

Agg, P. J., & Clary, D. C. 1991a, J. Chem. Phys., 95, 1037
Agg, P. J., & Clary, D. C. 1991b, Molec. Phys., 73, 317
Cernicharo, J., & Crovisier, J. 2005, Space Sci. Rev., 119, 29
Dabrowski, I. 1984, Canadian J. Phys., 62, 1639
Dubernet, M.-L., & Grosjean, A. 2002, A&A, 390, 793
Dubernet, M.-L., Tuckey, P. A., Jolicard, G., Michaut, X., & Berger, H. 2001, J. Chem. Phys., 114, 1286
Dubernet, M., Grosjean, A., Daniel, F., et al. 2006a, in Ro-vibrational Collisional Excitation Database: BASECOL – http://basecol.obspm.fr (Japan: Journal of Plasma and Fusion Research Series, series 7)
Dubernet, M.-L., Daniel, F., Grosjean, A., et al. 2006b, A&A, 460, 323
Faure, A., Valiron, P., Wernli, M., et al. 2005a, J. Chem. Phys., 122, 221102
Faure, A., Wiesenfeld, L., Wernli, M., & Valiron, P. 2005b, J. Chem. Phys., 123, 104309
Faure, A., Crimier, N., Ceccarelli, C., et al. 2007, A&A, 472, 1029
Green, S., Maluendes, S., & McLean, A. D. 1993, ApJS, 85, 181
Grosjean, A., Dubernet, M.-L., & Ceccarelli, C. 2003, A&A, 408, 1197
Heil, T. G., Kouri, D. J., & Green, S. 1978, J. Chem. Phys., 68, 2562
Hutson, J. M., & Green, S. 1994, MOLSCAT computer code,version 14 (United Kingdom: Collaborative Computational Project No. 6 of the Science and Engineering Research Council)
Kouri, D. J., Heil, T. G., & Shimoni, Y. 1976, J. Chem. Phys., 65, 1462
Kyrö, E. 1981, J. Mol. Spectrosc., 88, 167
Mandy, M. E., & Martin, P. G. 1993, ApJS, 86, 199
McBane, G. 2004, MOLSCAT computer code, parallel version (USA: G. McBane)
Melnick, G. J., Stauffer, J. R., Ashby, M. L. N., et al. 2000, ApJ, 539, L77
Noga, J., & Kutzelnigg, W. 1994, J. Chem. Phys., 101, 7738
Phillips, T. R., Maluendes, S., McLean, A. D., & Green, S. 1994, J. Chem. Phys., 101, 5824
Phillips, T. R., Maluendes, S., & Green, S. 1996, ApJS, 107, 467
Sandqvist, A., Bergman, P., Black, J. H., et al. 2003, A&A, 402, L63
Spinoglio, L., Codella, C., Benedettini, M., et al. 2001, The Promise of the Herschel Space Observatory, ed. G. L. Pilbratt, J. Cernicharo, A. M. Heras, T. Prusti, & R. Harris, ESA-SP, 460, 495
Tsuji, T. 2001, A&A, 376, L1
Wilson, C. D., Mason, A., Gregersen, E., et al. 2003, A&A, 402, L59
Wright, C. M., vanDishoeck, E. F., Black, J. H., et al. 2000, A&A, 358, 689